HHS Public Access

Author manuscript

Cancer Cell. Author manuscript; available in PMC 2016 September 14.

Published in final edited form as:

Cancer Cell. 2015 September 14; 28(3): 357–369. doi:10.1016/j.ccell.2015.08.003.

Loss of ATRX suppresses resolution of telomere cohesion to control recombination in ALT cancer cells

Mahesh Ramamoorthy and **Susan Smith***

Summary

The chromatin-remodeler ATRX is frequently lost in cancer cells that use ALT (alternative lengthening of telomeres) for telomere maintenance, but its function in telomere recombination is unknown. Here we show that loss of ATRX suppresses the timely resolution of sister telomere cohesion that normally occurs prior to mitosis. In the absence of ATRX, the histone variant macroH2A1.1 binds to the poly(ADP-ribose) polymerase tankyrase 1, preventing it from localizing to telomeres and resolving cohesion. The resulting persistent telomere cohesion promotes recombination between sister telomeres, while it suppresses inappropriate recombination between non-sisters. Forced resolution of sister telomere cohesion induces excessive recombination between non-homologs, genomic instability, and impaired cell growth, indicating the ATRX-macroH2A1.1-tankyrase axis as a potential therapeutic target in ALT tumors.

Graphical abstract

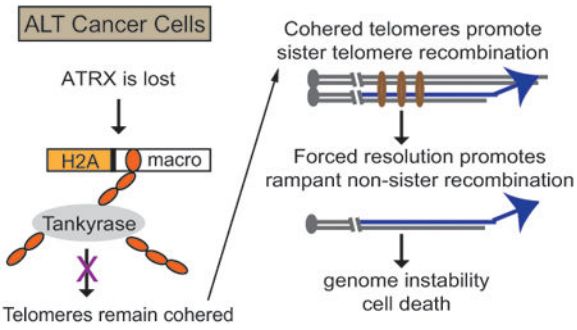

Keywords

telomeres; ALT alternative lengthening of telomeres; ATRX; tankyrase 1; recombination; cancer

*Corresponding author: Susan Smith, Kimmel Center for Biology and Medicine at the Skirball Institute, Department of Pathology, New York University School of Medicine, New York, NY 10016, Phone: 212-263-2540, Fax: 212-263-5711, susan.smith@med.nyu.edu.

Author Contributions: M.R. performed experiments. M.R. and S.S. designed experiments, interpreted the data, and wrote the manuscript.

Introduction

The unlimited replicative capacity of human tumor cells relies on their ability to counteract the progressive loss of telomeric DNA that accompanies cell division. Eighty-five to ninety percent of human cancers achieve this by up-regulating expression of telomerase, the enzyme that adds telomere repeats to chromosome ends by reverse transcription of an RNA template (Greider and Blackburn, 1985; Kim et al., 1994). The remaining 10 to 15 % of cancers activate ALT (alternative lengthening of telomeres) a recombination-based mechanism that extends telomere repeats using a telomeric DNA template (Bryan et al., 1997; Henson and Reddel, 2010). ALT cells exhibit significantly elevated rates of telomere sister-chromatid exchange (T-SCE) compared to SCE rates elsewhere in the genome. (Bechter et al., 2003; Londono-Vallejo et al., 2004). Such an increase is not observed in telomerase positive tumor cells, suggesting that ALT cells have lost the capacity to suppress homologous recombination at telomeres. Despite a large body of evidence indicating that hyperactive recombination underlies ALT, the mechanism that leads to activation of ALT is not known.

Recent studies revealed ATRX (α-thalassemia/mental retardation X-linked) as the protein most frequently lost in ALT tumors and ALT cell lines (Bower et al., 2012; Heaphy et al., 2011a; Heaphy et al., 2011b; Jiao et al., 2011; Lovejoy et al., 2012). ATRX is a SWI/SNF-like chromatin remodeler that has been implicated in a range of nuclear functions including gene expression, DNA replication, and histone variant deposition (Clynes et al., 2013; Ratnakumar and Bernstein, 2013). ATRX, along with its binding partner, the histone chaperone DAXX, is required for incorporation of the histone variant H3.3 into chromatin (Drane et al., 2010; Lewis et al., 2010). Mutations in DAXX and H3.3 are also found in ALT tumors (Heaphy et al., 2011a; Heaphy et al., 2011b; Jiao et al., 2011), strongly implicating the ATRX-DAXX-H3.3 histone deposition pathway in ALT. Additionally, loss of some other aspect of ATRX function is probably important, since ALT cells can harbor mutations in both ATRX/DAXX and H3.3 (Schwartzentruber et al., 2012). In contrast to its positive role in histone deposition, ATRX was found to act as a negative regulator of histone variant macroH2A incorporation into chromatin (Ratnakumar et al., 2012). Despite the absence of a clear mechanism for how loss of ATRX contributes to ALT, changes in chromatin organization and histone deposition are likely contributors (O'Sullivan and Almouzni, 2014). Consistent with this notion, a recent study demonstrated that depletion of the histone chaperone ASF1 led to induction of the ALT pathway (O'Sullivan et al., 2014).

Mammalian telomeres rely on the six subunit shelterin complex to mediate the specialized mechanisms required for their replication (Gilson and Geli, 2007; Stewart et al., 2012) protection (Palm and de Lange, 2008), and cohesion (Canudas et al., 2007; Canudas and Smith, 2009). Sister chromatids are cohered from the time of their replication in S phase until their separation at mitosis. Cohesion between sister chromatids provides a template for recombination and repair during and after DNA replication in S and G2 phases of the cell cycle (Sjogren and Nasmyth, 2001). Telomere cohesion is mediated by the cohesin subunit SA1 along with the shelterin subunits TRF1 and TIN2 (Canudas et al., 2007; Canudas and Smith, 2009; Remeseiro et al., 2012). Cohesion is particularly important at telomeres, which (due to their repetitive G-rich nature) pose extra burdens for the DNA replication machinery

(Gilson and Geli, 2007; Sfeir et al., 2009). The long length of ALT cell telomeres combined with other unique features, such as variant repeats that may not recruit sufficient shelterin (Conomos et al., 2012; Varley et al., 2002), exacerbate replication problems, but it is not known if ALT cells employ specialized mechanisms of cohesion to counter difficulties in telomere replication.

Resolution of telomere cohesion requires the TRF1-binding PARP, tankyrase 1 (Dynek and Smith, 2004). Tankyrase 1 PARsylates itself and TRF1 (Smith et al., 1998). Tankyrase 1 localizes to telomeres in late G2/early mitosis to resolve telomere cohesion (Bisht et al., 2013; Bisht et al., 2012). In tankyrase 1 depleted mitotic cells sister telomeres remain cohered, despite normal resolution of sister chromatid arms and centromeres (Dynek and Smith, 2004). Cells entering mitosis with cohered telomeres undergo a prolonged anaphase, but ultimately exit mitosis (Kim and Smith, 2014). Sister telomere cohesion can be rescued by wild type but not PARP dead tankyrase 1, indicating that a PARsylation dependent remodeling of telomeres is required (Bisht et al., 2013). Telomere cohesion is resolved prior to mitosis in normal human cells and telomerase positive cancer cells (Dynek and Smith, 2004; Hsiao and Smith, 2009), but the timing has not been investigated in ALT cells. Herein, we analyze the timing of telomere resolution and determine its impact on telomere recombination in ALT cancer cells.

Results

ATRX is required to resolve sister telomere cohesion

To determine the cohesion status of sister telomeres in ALT cells, we performed fluorescent is situ hybridization (FISH) using subtelomere specific probes. Cells were isolated by mitotic shake-off, fixed, and stained with a subtelomere probe 16p. As shown in Fig. 1A, telomeres of telomerase positive (non-ALT) tumor cells (HTC75 and HeLa) appear as doublets, indicating resolution of telomere cohesion. In contrast, in ALT tumor cells (U2OS, GM847, and VA13) telomeres appear as singlets, indicating cohered telomeres in mitosis (Fig. 1B and C). Similar results were obtained for 13q and 4P subtelomere probes (Fig. S1A and B). The observed persistent cohesion was unexpected since ALT cells contain similar levels of tankyrase 1 as telomerase positive cells (see Fig. 2E for example). Hence, we wondered if ALT cells might be deficient in other factors required to resolve telomere cohesion. Since loss of ATRX is a hallmark of ALT (Bower et al., 2012; Lovejoy et al., 2012), we asked if its reintroduction would restore resolution of telomere cohesion. Indeed, shown in Fig. 1D-F, expression of ATRX in ALT cells resolved the persistent telomere cohesion.

To determine if ATRX was required for resolution of cohesion in non-ALT cells, we depleted it from HeLa cells using siRNA. As shown in Fig. 1G-I for 16p (and in Fig. S1C and D for 13q), ATRX depletion led to persistent telomere cohesion in mitosis. Since this is the same phenotype observed upon tankyrase 1depletion (Dynek and Smith, 2004; Hsiao and Smith, 2009), we performed double depletion analysis to determine if ATRX and tankyrase 1 act in the same pathway. Depletion of tankyrase 1, ATRX, or the two together led to a similar persistent telomere cohesion phenotype (Fig. 1J-L). The absence of an

additive effect in the double knockdown suggests that ATRX and tankyrase 1 act in the same pathway.

MacroH2A1.1 is a common binding partner between tankyrase 1 and ATRX

We considered the possibility that tankyrase 1 and ATRX might associate indirectly through a common partner. We found (among the list of known ATRX-binding proteins) a plausible candidate, macroH2A1.1 (see schematic in Fig. 2A). MacroH2A is a histone variant comprised of an N-terminal H2A like domain and a C-terminal PAR-binding macro domain (Cantarino et al., 2013; Gamble and Kraus, 2010). It is found as three isoforms (macroH2A1.1, 1.2, and 2), but only one macroH2A1.1 (by virtue of an alternative splice) binds PAR (Kustatscher et al., 2005; Timinszky et al., 2009). The soluble pool of macroH2A was found to be associated with ATRX, which binds to the N-terminal H2A domain of all three isoforms (Ratnakumar et al., 2012). Since tankyrase 1 exists as an autoPARsylated protein in vivo (Cook et al., 2002; Smith and de Lange, 2000), we asked if macroH2A1.1 could serve as a common binding partner between ATRX and tankyrase 1.

First, we asked if macroH2A1.1 binds tankyrase 1 in vivo. As shown in Fig. 2B, transfected myc-epitope tagged macroH2A1.1 (but not macroH2A1.2) coimmunoprecipitated endogenous tankyrase 1 from HeLa cells. To determine if the interaction required the PAR modification on tankyrase 1, immunoprecipitation analysis was performed on U2OS cells stably expressing flag-tankyrase 1.WT or PARP-dead (PD) transfected with myc-macroH2A1.1 or.2. As shown in Fig. 2C, coimmunoprecipitation required the PARP activity of tankyrase 1 and occurred only with the macroH2A1.1 isoform, consistent with PAR-mediated binding. Coimmunoprecipitation analysis of the endogenous proteins further demonstrated a robust interaction between tankyrase 1 and macroH2A1 in U2OS cells (Fig. 2D).

We next asked if the interaction between tankyrase 1 and macroH2A1.1 was unique to ALT cells. Immunoblot analysis showed that (unlike ATRX) macroH2A1.1 (as well as tankyrase 1) were found in both ALT and telomerase positive cells (at varying levels) (Fig. 2E). For comparative immunoprecipitation analysis, we selected three cell lines in which the endogenous levels of macroH2A1.1 (and tankyrase 1) were similar: VA13, GM847, and HTC75. Immunoprecipitation of tankyrase 1 yielded coimmunoprecipitation of macroH2A1.1 from ALT cells (GM847 and VA13), but not from non-ALT (HTC75) cells (Fig. 2F), consistent with the notion that loss of ATRX in ALT cells rendered macroH2A1.1 available to bind tankyrase 1. Reintroduction of ATRX into ALT cells reduced the level of endogenous macroH2A1.1 that coimmunoprecipitated with endogenous tankyrase 1 (Fig. S2A and B) and effectively competed with endogenous tankyrase 1 for binding to overexpressed macroH2A1.1 (Fig. 2G). Together these studies suggest that loss of ATRX in ALT cells frees macroH2A1.1 to interact with tankyrase 1.

To directly measure the impact of excess macroH2A1 on tankyrase 1, we overexpressed macroH2A1.1 or macroH2A1.2 in HeLa cells and measured tankyrase 1 localization and function at telomeres. We showed previously using telomere chromatin immunoprecipitation analysis (ChIP) that tankyrase 1 localized to telomeres in G2/M phase of the cell cycle to resolve cohesion (Bisht et al., 2012). We thus asked if overexpression of

macroH2A1.1 would impact this localization. As shown in Fig. 2H and I, macroH2A1.1 (but not macroH2A1.2) led to a reduction in tankyrase 1 on telomeres. Telomere FISH analysis indicated that this reduction of tankyrase 1 at telomeres resulted in a concomitant block in resolution of sister telomere cohesion (Fig. 2J and K). Together these data suggest that macroH2A1.1 sequesters tankyrase 1, preventing its localization to and function at telomeres. Consistent with this notion, depletion of macroH2A1.1 in GM847 ALT cells led to resolution of persistent telomere cohesion (Fig. 2L and M).

Persistent telomere cohesion controls recombination in ALT cells

If, as our data suggests, tankyrase 1 in ALT cells is unavailable to resolve telomere cohesion due to its sequestration by macroH2A1.1, then overexpression of tankyrase 1 should rescue the persistent telomere cohesion phenotype. We used lentiviral infection to generate U2OS cell lines stably expressing a vector, flag-tankyrase 1.WT or tankyrase 1.PD and subjected them to telomere FISH analysis (Fig. 3A-C). Overexpression of tankyrase 1.WT, but not PD, rescued persistent sister telomere cohesion in ALT cells. To determine if loss of telomere cohesion influenced the high rate of telomere sister chromatid exchange (T-SCE) that is a feature of ALT (Bechter et al., 2003; Londono-Vallejo et al., 2004), cells were subjected to CO-FISH analysis (Bailey et al., 2001). As shown in Fig. 3D and E, overexpression of tankyrase 1.WT (but not PD) reduced the frequency of T-SCE, indicating that sister telomere cohesion regulates telomere recombination in ALT cells.

To determine if loss of telomere cohesion per se leads to reduced T-SCE, we took a different approach to resolve the persistent telomere cohesion in ALT cells. Previous studies showed that depletion of the shelterin subunit TIN2 or the cohesion subunit SA1 (but not SA2) prevented establishment/maintenance of sister telomere cohesion in HeLa cells (Canudas et al., 2007; Canudas and Smith, 2009). We thus depleted these proteins in U2OS ALT cells with siRNA, isolated cells by mitotic shake off, and analyzed telomere cohesion with a 16p probe (Fig. 3F-H). Depletion of TIN2 or SA1 rescued the persistent cohesion in ALT cells. Furthermore, CO-FISH analysis revealed a concomitant reduction in T-SCE (Fig. 3I and J), similar to what was observed above for tankyrase 1 overexpression. Together, these data show that persistent telomere cohesion in mitosis promotes sister telomere recombination in ALT cells.

Resolution of sister telomere cohesion leads to increased inter-telomeric copying

We observed a negative effect of tankyrase 1 overexpression on ALT cell growth. To analyze growth, U2OS cells were infected with tankyrase 1 lentiviruses, selected with puromycin, and the cell number determined on days 1 through 5. As shown in Figure 4A, tankyrase 1.WT (but not PD) showed no growth in the first four days. Many cells died following lentiviral infection and the surviving cells grew slowly, but ultimately recovered after 7 to 10 days of selection. Similar effects were observed in other ALT cell lines (VA13 and GM847, Fig. S3A and B), but not in HeLa cells (Fig. 4B), suggesting that forced resolution of telomere cohesion was detrimental to ALT cell growth.

We considered the possibility that upon resolution, freed sister telomeres would be available to invade non-sister telomeres. Studies in ALT cells showed that a telomere can copy a

telomere of a non-homologous chromosome (Dunham et al., 2000) and studies in telomerase negative mouse tumor cells demonstrated subtelomere copying of a non-homologous chromosome (Morrish and Greider, 2009). To assay for inter-telomere copying, we looked for an increase in the number of 16p subtelomere loci in tankyrase 1 overexpressing U2OS cells. As shown in Fig. 4C and D, while control cells never showed more than two sets of 16p loci, 8% of tankyrase 1.WT cells displayed 3 sets of 16p loci, suggesting that the 16p subtelomere was being copied to another chromosome. To determine if this copying could be detected as an overall increase in telomeric DNA, we performed telomere restriction fragment analysis and observed a slight increase in size and intensity of the telomere signal in tankyrase 1.WT cells (Fig. S3C).

To better measure intertelomeric copying we sought to follow the fate of a tagged telomere. For this we used a U2OS cell line (F6B2) harboring three stable integrations of bacterial lac operator (lacO) repeats directly adjacent to the 6q, 11p and 12q telomeres (Jegou et al., 2009). Expression of a GFP-LacI fusion protein allows visualization of the lacO tags (see schematic in Fig. 4E). F6B2(U2OS-3lacO)/GFPLacI cells were infected with lentiviruses expressing a vector control, tankyrase 1.WT, or tankyrase.PD, grown under selection for 7-10 days with puromycin, and analyzed for the number of lacO tags (Fig. 4F and G). Control cells generally displayed 3 tags. A small fraction had 4-5 tags. Tankyrase 1.WT cells showed a dramatic increase in telomere tags: a four-fold increase in cells with 4-5 tags and a ten-fold increase in cells with more than 5 tags. Tankyrase 1.PD cells were similar to the control, indicating that the increase in inter-telomere copying was dependent on the PARP domain. Measurement of DNA content by FACs analysis indicated that the increase in lacO tags in tankyrase 1.WT cells was not due to an increase in ploidy (Fig. S3D).

The macroH2A-binding domain of ATRX regulates telomere recombination

Our data suggest that persistent sister telomere cohesion serves an essential role in regulating recombination in ALT cells and further that loss of ATRX (a hallmark of ALT), frees macroH2A1.1 to sequester tankyrase 1 and prevent it from resolving sister telomere cohesion. Thus, introduction of the macroH2A1.1-binding domain of ATRX should recapitulate the effects seen with overexpression of tankyrase 1 (described above). Previous studies mapped the macroH2A1.1-binding domain to the first 841 amino acids of ATRX (Ratnakumar et al., 2012). First, we asked if this domain was able (like full length ATRX, see Fig. 2G) to compete with tankyrase 1 for macroH2A1.1 binding. Indeed, expression of ATRX.1-841 into U2OS cells effectively competed with tankyrase 1 for binding to macroH2A1.1 (Fig. 5A). To determine if this domain was sufficient to rescue persistent telomere cohesion, U2OS cells were transiently transfected with ATRX.1-841, isolated by mitotic shake-off, and analyzed by FISH with a 16p probe. As shown in Fig. 5B and C, ATRX.1-841 rescued persistent telomere cohesion. To determine the impact of ATRX on ALT cell growth, U2OS cells were infected with ATRX.1-841 or vector control lentiviruses, selected with puromycin, and the cell number determined on days 1 through 5. As shown in Figure 5D, ATRX.1-841 impaired cell growth. A similar effect was observed in ALT GM847 cells (Fig. S4A), but a lesser effect in non-ALT HeLa cells (Fig. S4B).

Next, we sought to further delimit the macroH2A-binding domain in ATRX. The N-terminus of ATRX contains an ATRX-DNMT3-DNMT3L (ADD) domain between amino acids 162-292 that binds histone H3 N-terminal tails (Dhayalan et al., 2011; Iwase et al., 2011) and is required for ATRX localization to heterochromatin. Coimmunoprecipitation analysis of deletion constructs shows that the macroH2A.1 binding activity resides in a domain (aa 322-841) of ATRX that is distinct from the ADD domain (Fig. 5E). FISH analysis of transiently transfected GM847 ALT cells showed that expression of ATRX. 322-841, is sufficient to resolve telomere cohesion (Fig. 5F and G) and to rescue persistent telomere cohesion induced by ATRX siRNA in HeLa cells (Fig. S4C and D).

Moreover, expression of ATRX.322-841 (like tankyrase 1 overexpression) led to a reduction in the frequency of T-SCE, measured by CO-FISH analysis (Fig. 5H) and to an increase in intertelomere copying, as measured by the number of 16p subtelomere loci per cell (Fig. 5I and J). Thirty per cent of ATRX.322-841 transfected cells versus 9% of control cells displayed 4 or more sets of 16p loci, indicating inter-telomeric copying. To confirm that the increase in loci was telomere-specific, we performed FISH analysis with a dual probe against the subtelomere and arm of the same chromosome (13q). As shown in Fig. 5K and L, we observed an increase in 13q telo (but not arm) loci, consistent with intertelomeric copying. Metaphase spread analysis shows that the extra 13q telo signals induced by ATRX are located at chromosome ends and further that the extra 13q telo signals are not accompanied by extra 13q arm signals and hence, are not due to endoreduplication or aneuploidy (Fig. S4E). We also measured the impact of ATRX expression using the lacO tag assay. F6B2(U2OS-3lacO) cells were transiently transfected with GFPLacI and FlagATRX.322-841 or FlagATRX.1-321 (as a control) and Flag-expressing cells were scored for lacO tags. As shown in Fig. 5M and N, FlagATRX.1-321 (which does not bind macroH2A1.1) had no effect and was similar to vector control (see Fig. 4G), whereas ATRX.322-841 induced copying of the lacO telomere tags. Similar results were obtained by expression of full-length ATRX (Fig. S4F and G). Finally, consistent with the notion that ATRX induces telomere copying by binding and sequestering macroH2A1.1, we found that depletion of macroH2A1.1 led to a decrease in T-SCE (measured by CO-FISH) (Fig. S4H) and induced intertelomere copying shown by an increase in 16p telomere loci (Fig. S4I and J) and an increase in lacO telomere tags (Fig. S4K and L).

Loss of telomere cohesion leads to rampant, immediate inter-telomere recombination

In the experiments described above, inter-telomere copying was detected within a very short time frame (only 18 hr after transfection with ATRX), suggesting a rapid induction of recombination. This prompted us to evaluate the immediate impact of sister telomere resolution (induced by tankyrase 1 overexpression) on telomere tag copying. Rather than analyzing F6B2(U2OS-3lacO)/GFPLacI selected cells 7-10 days after lentiviral infection (as shown in Fig. 4), cells were infected and analyzed (without selection) on Day 1, 2, 3, and 4 for lacO tags. We found an immediate, dramatic effect. As shown in (Fig. 6A and B), on Day 1 nearly 60% of tankyrase 1 overexpressing cells (compared to 0% of control cells) had more than 5 lacO tags, indicating an initial burst of telomere copying immediately following tankyrase 1 overexpression. The frequency of lacO tags declined gradually over the next 2 to 4 days (Fig. 6C and Fig. S5A), as did the levels of tankyrase 1 protein (Fig. S5B),

suggesting that cells could not survive the rampant telomere copying induced by tankyrase 1 overexpression. FACs analysis indicated no cell cycle arrest, just a slight increase in the S and G_2/M populations on Day 1 (Fig. S5C) (consistent with increased recombination) and annexin V staining showed a three-fold increase in apoptosis (Fig. S5D) in tankyrase 1 overexpressing cells.

Consistent with an increase in recombination, we observed a two-fold increase in RAD51 (a marker for homologous recombination) foci on Day 1 that gradually declined over days 2 to 4 (Fig. 6D and E). To determine if the recombination that was unleashed by tankyrase 1 (and resolution of telomere cohesion) was dependent on RAD51, we used the small molecule RAD51 inhibitor RI-1 (Budke et al., 2012). As shown in Fig. 6F and G, RI-1 prevented induction of RAD51 foci in tankyrase overexpressing U2OS cells and it blocked tankyrase 1 induced recombination (measured by lacO tags) in F6B2(U2OS-3lacO)/GFPLacI cells (Fig. 6H and I). Interestingly, a recent study demonstrated that RAD51 was required for interchromosomal homology searches initiated by damaged telomeres in ALT cells (Cho et al., 2014). Our results show that RAD51 is required for interchromosomal copying of tagged telomeres induced by loss of sister telomere cohesion.

Finally, to determine if this recombination impacted genome stability, cells were analyzed for the presence of micronuclei. As shown in Fig. 6J and K, we observed a 3-fold increase in micronuclei on Day 2 in U2OS (and in U2OS lacO/GFPLacI cells; Fig. S5E) that follows the burst of recombination on Day 1 and remains elevated over days 3 and 4.

Discussion

Loss of ATRX is a hallmark of ALT cells. Our studies have uncovered a critical role for loss of ATRX in suppressing resolution of sister telomere cohesion. In ALT cells (in the absence of ATRX) tankyrase 1 is bound by macroH2A1.1 and thereby prevented from resolving telomere cohesion. When ATRX is introduced into ALT cells it binds macroH2A1.1, freeing tankyrase 1 to resolve cohesion (see model in Fig. 7A). In ALT cells sister telomeres remain cohered into mitosis. Under these conditions the sister telomere is the favored copy template and cells undergo high rates of T-SCE. Upon forced resolution of sister telomere cohesion (by introduction of ATRX, overexpression of tankyrase 1, or depletion of macroH2A1.1) sister telomeres are freed from each other and any telomere can be the copy template (see model in Fig. 7B). Hence, persistent telomere cohesion serves a critical dual role in ALT; it promotes recombination between sister telomeres that is important for DNA repair and telomere maintenance, while it prevents excessive recombination between non-sister telomeres that is detrimental to cell growth.

Previous studies show that ALT cell telomeres copy DNA from telomeric templates; copying of subtelomeres was not detected (Dunham et al., 2000). This copying occurs at low frequency; it is detected by analyzing cells carried for multiple generations. The copying that we observe here, upon forced resolution of cohesion, differs from the normal ALT cell copying in at least two ways: it occurs between sub telomeres and it occurs rapidly, within 18 to 24 hours of overexpression of tankyrase 1 or introduction of ATRX. Interestingly, copying of subtelomeres has been observed previously at high frequency, not in ALT cells,

but in cells from late-generation telomerase-null mouse Eμmyc$^+$ tumors with short telomeres (Morrish and Greider, 2009). The authors suggest that degradation of short telomeres into subtelomeres could lead to strand invasion and copying. Similarly, we suggest that ALT cell telomeres, which can be very short as evidenced by chromosome ends with no detectable telomere signal (Henson et al., 2002), could (upon forced resolution of cohesion) become available to invade and copy subtelomeres of other chromosomes.

ATRX impacts tankyrase 1 function and sister telomere cohesion through its macroH2A binding domain, which is distinct from its ADD, DAXX binding, and ATPase domains. While the DAXX/H3.3 axis of ATRX is most strongly implicated in ALT, the observation that some ALT tumors have mutations in both ATRX and H3.3 (the cargo of DAXX deposition), points to a role for ATRX in addition to its DAXX/H3.3 histone chaperone function. Moreover, ALT is usually accompanied by the absence of detectable levels of ATRX protein, even without obvious changes in the ATRX gene (Bower et al., 2012; Heaphy et al., 2011a; Lovejoy et al., 2012). This might be explained by the need to lose the N-terminal macroH2A-binding domain to promote persistent telomere cohesion. We speculate that elimination of at least two axes of ATRX may be required for ALT. Loss of the ATRX-DAXX-H3.3 axis could lead to epigenetic changes at telomeres that render them permissive for recombination, while at the same time loss of the ATRX-macroH2A1.1-tankryase axis would be essential to control the hyper recombination phenotype.

Despite the mounting evidence linking ATRX to ALT, the crucial demonstration of a causal role for ATRX in activation of ALT has not been reported. Indeed, knockdown of ATRX in HeLa cells or SV40 immortalized BJ fibroblasts was not sufficient to convert them to the ALT cell state (Lovejoy et al., 2012; O'Sullivan et al., 2014). However, it is possible that the sequence of events required for ALT activation was not recapitulated in these experiments. Loss of ATRX may be required as an early event, prior to transformation. Interestingly, persistent telomere cohesion in mitosis (like the kind reported in this study) has also been observed in aging human fibroblasts in culture just prior to senescence (Kim and Smith, 2014; Ofir et al., 2002; Yalon et al., 2004). Although the mechanism is not known, (it could be due to reduction of ATRX or to other changes that influence telomere cohesion), it raises the possibility that the precondition of persistent telomere cohesion might favor activation of the ALT pathway over up-regulation of telomerase during tumorigenesis. This could be tested by using human fibroblasts with persistent telomere cohesion (generated by ATRX or tankyrase 1 depletion) as a starting point for SV40 transformation and asking if ALT is then the preferred choice for telomere maintenance.

Our observation that restoring normal resolution of telomere cohesion to ALT cells leads to genomic instability and impaired cell growth, suggests an opportunity for ALT cell specific tumor therapy. We demonstrated restoration of telomere cohesion by introduction of either full length ATRX or (with similar efficiency) the macroH2A-binding domain of ATRX. Surprisingly, although the ATRX and tankyrase binding domains of macroH2A1.1 are distinct, we found that binding of ATRX to macroH2A1.1 led to release of tankyrase 1, suggesting that ATRX binding might induce a conformational change in macroH2A1.1 that releases tankyrase 1. Hence, it will be important to further define the macroH2A-binding domain of ATRX with the potential goal of identifying a peptide or small molecule that can

bind to macroH2A1.1 and free tankyrase 1 to resolve cohesion. Another target could be the PAR-binding domain of macroH2A1.1. Here structural studies have already elucidated the binding of NAD^+ metabolites such as ADP-ribose and O-acetyl-ADP-ribose (Kustatscher et al., 2005), raising the possibility that small molecules that disrupt the interface between macroH2A1.1 and PARsylated tankyrase 1 can be identified.

The notion that the ALT cell phenotype is driven by a recombination-based mechanism was well established. However, what was heretofore unappreciated was the level to which that recombination would occur if it were not restrained by persistent telomere cohesion. Our demonstration, that forced resolution of sister telomere cohesion can unleash the hyper-recombination and promote ALT cell death, suggests a viable ALT-specific anti-cancer strategy.

Experimental Procedures

Cell lines

ALT cancer cell lines [U2OS, WI38-VA13/2RA (VA13), and GM847] and telomerase positive cancer cell lines [HeLa1.2.11(van Steensel et al., 1998) and HTC75(van Steensel and de Lange, 1997)] were grown under standard conditions. F6B2 a neomycin resistant U2OS cell line that has three stably integrated lacO arrays directly adjacent to the telomeres of chromosomes 6q, 11p and 12q (Jegou et al., 2009) was a gift from Karsten Rippe). The F6B2(U2OS-3lacO)/GFPLacI cell line was generated by transfection of F6B2 with a GFPLacI plasmid, p3'ss-gfp-Lac-NLS (Robinett et al., 1996). Cells were selected with 75 μg/ml hygromycin and surviving clones were propagated by alternating weekly growth in 75 μg/ml hygromycin and 750 μg/ml G418.

Where indicated RAD51 inhibitor RI-1 (Selleckchem) was dissolved in DMSO and add to the culture medium 8 hr prior to harvest at a final concentration of 20 μM.

Lentiviral infection—Lentiviruses were produced by transfection of 293FT (Invitrogen) packaging cells with a three-plasmid system as described previously (Naldini et al., 1996; Zufferey et al., 1997). 293FT cells were seeded in a 6-cm dish at 1.2×10^6 cells and 24 hr later were transfected with 1 μg lentiviral vector, 1 μg pCMVΔR.89 packaging plasmid, and 100 ng pMD.G envelope plasmid using Lipofectamine 2000 (Invitrogen) according to the manufacturer's instructions. Lentiviral supernatants were collected at 48 hr after transfection, filtered with a 0.45-μm filter (Millipore), and frozen at -80°C. Twenty-four hr before infection, target cells were seeded at a density of 2.2×10^5. Target cells were infected for 48-72 hr with lentiviral supernatants supplemented with 8 μg/ml polybrene (Sigma-Aldrich). Cells were sub-cultured 1:2 into medium containing 2 μg/ml puromycin and upon confluence (approximately 48 hr later) were designated as population doubling (PD) 0. For tankyrase 1.WT cells confluence (PD 0) was reached in 7 to 10 days and cells continued to grow slowly, but eventually recovered at around PD2. For macroH2A1 shRNA, cells were subcultured into medium containing 2 μg/ml puromycin and harvested for analysis 24 hours later.

For growth curve analyses, target cells were infected for 48-72 hr, sub-cultured 1:2 into medium containing 2 μg/ml puromycin, and grown for 48 hr. Cells were counted and plated into 6 wells in medium containing 2 μg/ml puromycin. The next day (day 0) cells were harvested and counted using a haemocytometer and used to normalize the number of cells plated. Cells were then harvested and counted every 24 hr over the next 5 days. Cell numbers were calculated as a ratio of the day 0 counts.

For the time course analysis, target cells were infected for 48-72 hr, sub-cultured 1:2 into medium containing 2 μg/ml puromycin and grown for 24 hr. Cells were seeded into medium without puromycin on cover slips (for immunofluorescence) and in wells (for FACS and for Annexin V staining) and analyzed every 24 hr for the next 4 days.

Chromosome specific FISH

Cells were fixed and processed as described previously (Dynek and Smith, 2004). Briefly, cells were isolated by mitotic shake-off, fixed twice in methanol:acetic acid (3:1) for 15 min, cytospun (Shandon Cytospin) at 2000 rpm for 2 min onto slides, rehydrated in 2× SSC at 37°C for 2 min, and dehydrated in an ethanol series of 70%, 80% and 95% for 2 min each. Cells were denatured at 75°C for 2 min and hybridized overnight at 37°C with subtelomeric FITC-conjugated (16ptelo, 13qtelo, or 4ptelo) and TRITC-conjugated 13q14.3 deletion (arm) probes from Cytocell. Cells were washed in 0.4× SSC at 72°C for 2 min, and in 2× SSC with 0.05% Tween 20 at RT for 30 s. DNA was stained with 0.2 μg/ml DAPI. Mitotic cells were scored as having telomeres cohered if 50% or more of their loci appeared as singlets, i.e. one out of two or two out of three. In U2OS cells stained with 16ptelo ∼40 % had one locus and ∼60% two loci; only cells with two loci were scored.

Indirect immunofluorescence

For staining lacO tags, lentivirally infected U2OS-lacO/GFPLacI cells were fixed in 2% paraformaldehyde in phosphate-buffered saline (PBS) for 10 min at room temperature (RT), permeabilized in 0.5% NP40/PBS buffer for 10 min at RT, blocked in 1% bovine serum albumin (BSA) in PBS, and incubated with rabbit anti-GFP (1:500) (Abcam, 290). For staining RAD51 foci, lentivirally infected U2OS cells were permeabilized in Triton X-100 buffer (0.5% Triton X-100, 20 mM Hepes-KOH at pH 7.9, 50 mM NaCl, 3 mM MgCl2, 300 mM sucrose) for 5 min at RT and fixed in 3% paraformaldehyde (in PBS, 2% sucrose) for 10 min at RT, followed by permeabilization in Triton X-100 buffer for 10 min RT. Cells were blocked in 1% BSA/PBS, followed by incubation with rabbit anti-RAD51 (4 μg/ml) (Santa Cruz Biotechnology, 8349). Primary antibodies were detected with fluorescein isothiocyanate-conjugated donkey anti-rabbit antibodies (1:100) (Jackson Laboratories). DNA was stained with DAPI (0.2 μg/ml) to score micronuclei.

Image Acquisition

Images were acquired using a microscope (Axioplan 2; Carl Zeiss, Inc.) with a Plan Apochrome 63× NA 1.4 oil immersion lens (Carl Zeiss, Inc.) and a digital camera (C4742-95; Hamamatsu Photonics). Images were acquired and processed using Openlab software (Perkin Elmer).

Statistical Analysis

Statistical analysis was performed using Prism 6 software. Student's unpaired t-test was applied. Data are shown as mean ±SEM (standard error of the mean) or as mean ±SD (standard deviation); $P<0.05$ values were considered significant.

Supplementary Material

Refer to Web version on PubMed Central for supplementary material.

Acknowledgments

We thank Karsten Rippe for the F6B2 cell line and Junjie Chen for the ATRX plasmid. Research reported in this publication was supported by the National Cancer Institute of the National Institutes of Health under award number R01CA116352 and by NYSTEM CO28123.

References

Bailey SM, Cornforth MN, Kurimasa A, Chen DJ, Goodwin EH. Strand-specific postreplicative processing of mammalian telomeres. Science. 2001; 293:2462–2465. [PubMed: 11577237]

Bechter OE, Zou Y, Shay JW, Wright WE. Homologous recombination in human telomerase-positive and ALT cells occurs with the same frequency. EMBO Rep. 2003; 4:1138–1143. [PubMed: 14618159]

Bisht KK, Daniloski Z, Smith S. SA1 binds directly to DNA through its unique AT-hook to promote sister chromatid cohesion at telomeres. J Cell Sci. 2013; 126:3493–3503. [PubMed: 23729739]

Bisht KK, Dudognon C, Chang WG, Sokol ES, Ramirez A, Smith S. GDP-mannose-4,6-dehydratase is a cytosolic partner of tankyrase 1 that inhibits its poly(ADP-ribose) polymerase activity. Mol Cell Biol. 2012; 32:3044–3053. [PubMed: 22645305]

Bower K, Napier CE, Cole SL, Dagg RA, Lau LM, Duncan EL, Moy EL, Reddel RR. Loss of wild-type ATRX expression in somatic cell hybrids segregates with activation of Alternative Lengthening of Telomeres. PloS one. 2012; 7:e50062. [PubMed: 23185534]

Bryan TM, Englezou A, Dalla-Pozza L, Dunham MA, Reddel RR. Evidence for an alternative mechanism for maintaining telomere length in human tumors and tumor-derived cell lines [see comments]. Nat Med. 1997; 3:1271–1274. [PubMed: 9359704]

Budke B, Logan HL, Kalin JH, Zelivianskaia AS, Cameron McGuire W, Miller LL, Stark JM, Kozikowski AP, Bishop DK, Connell PP. RI-1: a chemical inhibitor of RAD51 that disrupts homologous recombination in human cells. Nucleic Acids Res. 2012; 40:7347–7357. [PubMed: 22573178]

Cantarino N, Douet J, Buschbeck M. MacroH2A--an epigenetic regulator of cancer. Cancer Lett. 2013; 336:247–252. [PubMed: 23531411]

Canudas S, Houghtaling BR, Kim JY, Dynek JN, Chang WG, Smith S. Protein requirements for sister telomere association in human cells. Embo J. 2007; 26:4867–4878. [PubMed: 17962804]

Canudas S, Smith S. Differential regulation of telomere and centromere cohesion by the Scc3 homologues SA1 and SA2, respectively, in human cells. J Cell Biol. 2009; 187:165–173. [PubMed: 19822671]

Cho NW, Dilley RL, Lampson MA, Greenberg RA. Interchromosomal homology searches drive directional ALT telomere movement and synapsis. Cell. 2014; 159:108–121. [PubMed: 25259924]

Clynes D, Higgs DR, Gibbons RJ. The chromatin remodeller ATRX: a repeat offender in human disease. Trends Biochem Sci. 2013; 38:461–466. [PubMed: 23916100]

Conomos D, Stutz MD, Hills M, Neumann AA, Bryan TM, Reddel RR, Pickett HA. Variant repeats are interspersed throughout the telomeres and recruit nuclear receptors in ALT cells. J Cell Biol. 2012; 199:893–906. [PubMed: 23229897]

Cook BD, Dynek JN, Chang W, Shostak G, Smith S. Role for the related poly(ADP-Ribose) polymerases tankyrase 1 and 2 at human telomeres. Mol Cell Biol. 2002; 22:332–342. [PubMed: 11739745]

Dhayalan A, Tamas R, Bock I, Tattermusch A, Dimitrova E, Kudithipudi S, Ragozin S, Jeltsch A. The ATRX-ADD domain binds to H3 tail peptides and reads the combined methylation state of K4 and K9. Hum Mol Genet. 2011; 20:2195–2203. [PubMed: 21421568]

Drane P, Ouararhni K, Depaux A, Shuaib M, Hamiche A. The death-associated protein DAXX is a novel histone chaperone involved in the replication-independent deposition of H3.3. Genes Dev. 2010; 24:1253–1265. [PubMed: 20504901]

Dunham MA, Neumann AA, Fasching CL, Reddel RR. Telomere maintenance by recombination in human cells. Nat Genet. 2000; 26:447–450. [PubMed: 11101843]

Dynek JN, Smith S. Resolution of sister telomere association is required for progression through mitosis. Science. 2004; 304:97–100. [PubMed: 15064417]

Gamble MJ, Kraus WL. Multiple facets of the unique histone variant macroH2A: from genomics to cell biology. Cell Cycle. 2010; 9:2568–2574. [PubMed: 20543561]

Gilson E, Geli V. How telomeres are replicated. Nat Rev Mol Cell Biol. 2007; 8:825–838. [PubMed: 17885666]

Greider CW, Blackburn EH. Identification of a specific telomere terminal transferase activity in Tetrahymena extracts. Cell. 1985; 43:405–413. [PubMed: 3907856]

Heaphy CM, de Wilde RF, Jiao Y, Klein AP, Edil BH, Shi C, Bettegowda C, Rodriguez FJ, Eberhart CG, Hebbar S, et al. Altered telomeres in tumors with ATRX and DAXX mutations. Science. 2011a; 333:425. [PubMed: 21719641]

Heaphy CM, Subhawong AP, Hong SM, Goggins MG, Montgomery EA, Gabrielson E, Netto GJ, Epstein JI, Lotan TL, Westra WH, et al. Prevalence of the alternative lengthening of telomeres telomere maintenance mechanism in human cancer subtypes. The American journal of pathology. 2011b; 179:1608–1615. [PubMed: 21888887]

Henson JD, Neumann AA, Yeager TR, Reddel RR. Alternative lengthening of telomeres in mammalian cells. Oncogene. 2002; 21:598–610. [PubMed: 11850785]

Henson JD, Reddel RR. Assaying and investigating Alternative Lengthening of Telomeres activity in human cells and cancers. FEBS letters. 2010; 584:3800–3811. [PubMed: 20542034]

Hsiao SJ, Smith S. Sister telomeres rendered dysfunctional by persistent cohesion are fused by NHEJ. J Cell Biol. 2009; 184:515–526. [PubMed: 19221198]

Iwase S, Xiang B, Ghosh S, Ren T, Lewis PW, Cochrane JC, Allis CD, Picketts DJ, Patel DJ, Li H, Shi Y. ATRX ADD domain links an atypical histone methylation recognition mechanism to human mental-retardation syndrome. Nature structural & molecular biology. 2011; 18:769–776.

Jegou T, Chung I, Heuvelman G, Wachsmuth M, Gorisch SM, Greulich-Bode KM, Boukamp P, Lichter P, Rippe K. Dynamics of telomeres and promyelocytic leukemia nuclear bodies in a telomerase-negative human cell line. Mol Biol Cell. 2009; 20:2070–2082. [PubMed: 19211845]

Jiao Y, Shi C, Edil BH, de Wilde RF, Klimstra DS, Maitra A, Schulick RD, Tang LH, Wolfgang CL, Choti MA, et al. DAXX/ATRX, MEN1, and mTOR pathway genes are frequently altered in pancreatic neuroendocrine tumors. Science. 2011; 331:1199–1203. [PubMed: 21252315]

Kim MK, Smith S. Persistent telomere cohesion triggers a prolonged anaphase. Mol Biol Cell. 2014; 25:30–40. [PubMed: 24173716]

Kim NW, Piatyszek MA, Prowse KR, Harley CB, West MD, Ho PL, Coviello GM, Wright WE, Weinrich SL, Shay JW. Specific association of human telomerase activity with immortal cells and cancer [see comments]. Science. 1994; 266:2011–2015. [PubMed: 7605428]

Kustatscher G, Hothorn M, Pugieux C, Scheffzek K, Ladurner AG. Splicing regulates NAD metabolite binding to histone macroH2A. Nature structural & molecular biology. 2005; 12:624–625.

Lewis PW, Elsaesser SJ, Noh KM, Stadler SC, Allis CD. Daxx is an H3.3-specific histone chaperone and cooperates with ATRX in replication-independent chromatin assembly at telomeres. Proc Natl Acad Sci U S A. 2010; 107:14075–14080. [PubMed: 20651253]

Londono-Vallejo JA, Der-Sarkissian H, Cazes L, Bacchetti S, Reddel RR. Alternative lengthening of telomeres is characterized by high rates of telomeric exchange. Cancer Res. 2004; 64:2324–2327. [PubMed: 15059879]

Lovejoy CA, Li W, Reisenweber S, Thongthip S, Bruno J, de Lange T, De S, Petrini JH, Sung PA, Jasin M, et al. Loss of ATRX, genome instability, and an altered DNA damage response are hallmarks of the alternative lengthening of telomeres pathway. PLoS genetics. 2012; 8:e1002772. [PubMed: 22829774]

Morrish TA, Greider CW. Short telomeres initiate telomere recombination in primary and tumor cells. PLoS genetics. 2009; 5:e1000357. [PubMed: 19180191]

Naldini L, Blomer U, Gallay P, Ory D, Mulligan R, Gage FH, Verma IM, Trono D. In vivo gene delivery and stable transduction of nondividing cells by a lentiviral vector. Science. 1996; 272:263–267. [PubMed: 8602510]

O'Sullivan RJ, Almouzni G. Assembly of telomeric chromatin to create ALTernative endings. Trends Cell Biol. 2014; 24:675–685. [PubMed: 25172551]

O'Sullivan RJ, Arnoult N, Lackner DH, Oganesian L, Haggblom C, Corpet A, Almouzni G, Karlseder J. Rapid induction of alternative lengthening of telomeres by depletion of the histone chaperone ASF1. Nature structural & molecular biology. 2014; 21:167–174.

Ofir R, Yalon-Hacohen M, Segev Y, Schultz A, Skorecki KL, Selig S. Replication and/or separation of some human telomeres is delayed beyond S-phase in pre-senescent cells. Chromosoma. 2002; 111:147–155. [PubMed: 12355203]

Palm W, de Lange T. How shelterin protects mammalian telomeres. Annu Rev Genet. 2008; 42:301–334. [PubMed: 18680434]

Ratnakumar K, Bernstein E. ATRX: the case of a peculiar chromatin remodeler. Epigenetics: official journal of the DNA Methylation Society. 2013; 8:3–9.

Ratnakumar K, Duarte LF, LeRoy G, Hasson D, Smeets D, Vardabasso C, Bonisch C, Zeng T, Xiang B, Zhang DY, et al. ATRX-mediated chromatin association of histone variant macroH2A1 regulates alpha-globin expression. Genes Dev. 2012; 26:433–438. [PubMed: 22391447]

Remeseiro S, Cuadrado A, Carretero M, Martinez P, Drosopoulos WC, Canamero M, Schildkraut CL, Blasco MA, Losada A. Cohesin-SA1 deficiency drives aneuploidy and tumourigenesis in mice due to impaired replication of telomeres. EMBO J. 2012; 31:2076–2089. [PubMed: 22415365]

Robinett CC, Straight A, Li G, Willhelm C, Sudlow G, Murray A, Belmont AS. In vivo localization of DNA sequences and visualization of large-scale chromatin organization using lac operator/repressor recognition. J Cell Biol. 1996; 135:1685–1700. [PubMed: 8991083]

Schwartzentruber J, Korshunov A, Liu XY, Jones DT, Pfaff E, Jacob K, Sturm D, Fontebasso AM, Quang DA, Tonjes M, et al. Driver mutations in histone H3.3 and chromatin remodelling genes in paediatric glioblastoma. Nature. 2012; 482:226–231. [PubMed: 22286061]

Sfeir A, Kosiyatrakul ST, Hockemeyer D, MacRae SL, Karlseder J, Schildkraut CL, de Lange T. Mammalian telomeres resemble fragile sites and require TRF1 for efficient replication. Cell. 2009; 138:90–103. [PubMed: 19596237]

Sjogren C, Nasmyth K. Sister chromatid cohesion is required for postreplicative double-strand break repair in Saccharomyces cerevisiae. Curr Biol. 2001; 11:991–995. [PubMed: 11448778]

Smith S, de Lange T. Tankyrase promotes telomere elongation in human cells. Currrent Biology. 2000; 10:1299–1302.

Smith S, Giriat I, Schmitt A, de Lange T. Tankyrase, a poly(ADP-ribose) polymerase at human telomeres [see comments]. Science. 1998; 282:1484–1487. [PubMed: 9822378]

Stewart JA, Chaiken MF, Wang F, Price CM. Maintaining the end: roles of telomere proteins in end-protection, telomere replication and length regulation. Mutat Res. 2012; 730:12–19. [PubMed: 21945241]

Timinszky G, Till S, Hassa PO, Hothorn M, Kustatscher G, Nijmeijer B, Colombelli J, Altmeyer M, Stelzer EH, Scheffzek K, et al. A macrodomain-containing histone rearranges chromatin upon sensing PARP1 activation. Nature structural & molecular biology. 2009; 16:923–929.

van Steensel B, de Lange T. Control of telomere length by the human telomeric protein TRF1. Nature. 1997; 385:740–743. [PubMed: 9034193]

van Steensel B, Smogorzewska A, de Lange T. TRF2 protects human telomeres from end-to-end fusions. Cell. 1998; 92:401–413. [PubMed: 9476899]

Varley H, Pickett HA, Foxon JL, Reddel RR, Royle NJ. Molecular characterization of inter-telomere and intra-telomere mutations in human ALT cells. Nat Genet. 2002; 30:301–305. [PubMed: 11919561]

Yalon M, Gal S, Segev Y, Selig S, Skorecki KL. Sister chromatid separation at human telomeric regions. J Cell Sci. 2004; 117:1961–1970. [PubMed: 15039457]

Zufferey R, Nagy D, Mandel RJ, Naldini L, Trono D. Multiply attenuated lentiviral vector achieves efficient gene delivery in vivo. Nature biotechnology. 1997; 15:871–875.

Significance

Cancer cells achieve immortality by upregulating telomerase or by activating ALT (alternative lengthening of telomeres), a recombination-based mechanism. Since ALT is activated in 10-15 % of human tumors and it may provide an adaptive mechanism to anti-telomerase therapies, it is an important target for anticancer strategies. The chromatin-remodeler ATRX is frequently lost in ALT, but its function in telomere recombination is unknown. Here we show that loss of ATRX suppresses the timely resolution of sister telomere cohesion that normally occurs prior to mitosis. The resulting persistent telomere cohesion promotes chromatid exchange between sister telomeres, while it suppresses inappropriate recombination between non-sisters. Forced resolution of cohesion unleashes excessive recombination and impairs ALT cell growth, suggesting a therapeutic strategy for ALT tumors.

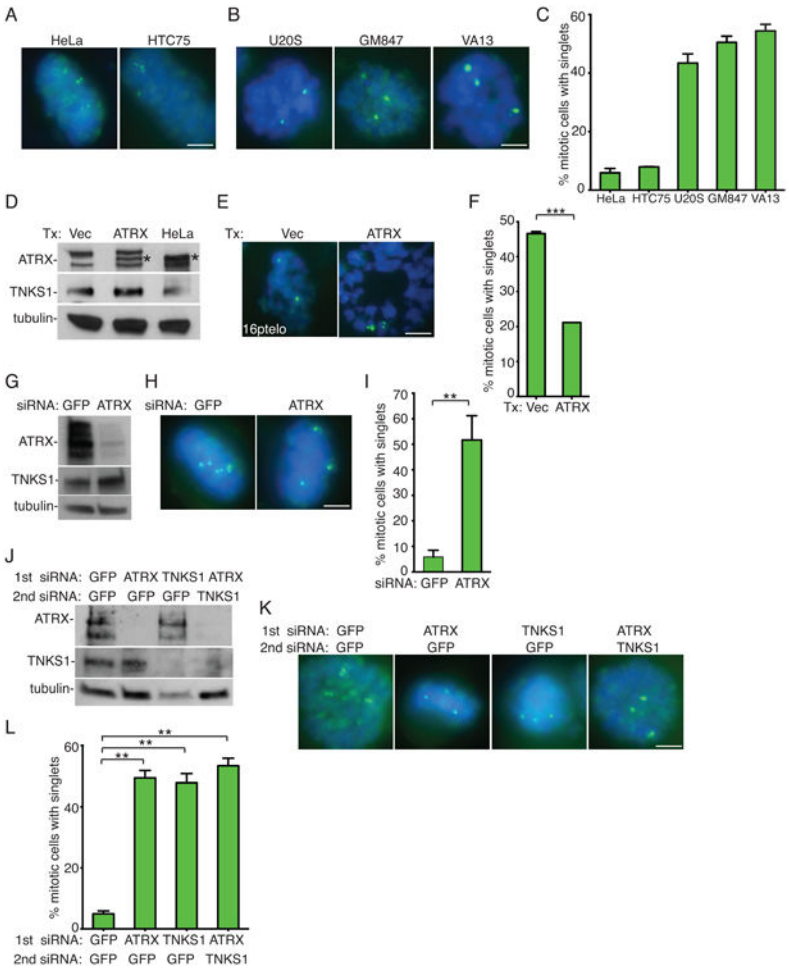

Figure 1.

ATRX is required for resolution of sister telomere cohesion. (A, B) FISH analysis of non-ALT (A) and ALT (B) mitotic cells with a 16ptelo probe (green). (C) Quantification of the frequency of mitotic cells with cohered telomeres. Average of two independent experiments (n=50-99 cells each) ±SEM. (D) Immunoblot analysis of transfected U2OS cell extracts and (as a control for ATRX protein) HeLa cell extracts; * indicates the ATRX specific band. (E) FISH analysis of vector or ATRX-transfected U2OS mitotic cells with a 16ptelo probe (green). (F) Quantification of the frequency of mitotic cells with cohered telomeres. Average of two independent experiments (n=50-53 cells each) ±SEM. (G) Immunoblot analysis of siRNA-treated HeLa cell extracts. (H) FISH analysis of GFP or ATRX siRNA-treated HeLa mitotic cells with a 16ptelo probe (green). (I) Quantification of the frequency of mitotic cells with cohered telomeres. Average of three independent experiments (n=34-64 cells each) ±SD. (J) Immunoblot analysis of siRNA treated HeLa cell extracts. (K) FISH analysis of the indicated double siRNA-treated HeLa mitotic cells using a 16ptelo probe (green). (L) Quantification of the frequency of mitotic cells with cohered telomeres. Average of two independent experiments (n=49-51 cells each) ±SEM. (A, B, E, H, and K) DNA was stained with DAPI (blue). Scale bars, 5 μm. **p≤0.01, ***p≤0.001, students unpaired t-test. See also Figure S1.

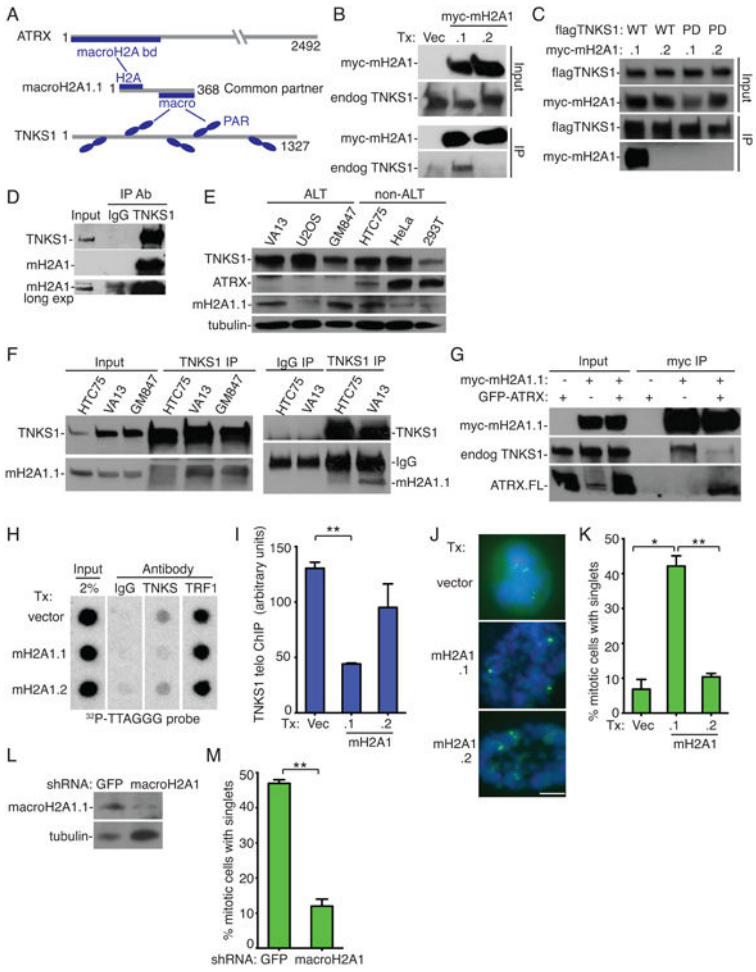

Figure 2.

MacroH2A1.1 is a common partner of ATRX and tankyrase 1 that mediates telomere cohesion in ALT cells. (A) Schematic diagram of macroH2A1.1 as a common binding partner between ATRX and tankyrase 1 (TNKS1). (B) Immunoblot analysis of transfected HeLa cell extracts following immunoprecipitation with anti-myc antibody. (C) Immunoblot analysis of transfected U2OS cell extracts following immunoprecipitation with anti-flag antibody. (D) Immunoblot analysis of U2OS cell extracts following immunoprecipitation with anti-TNKS1 antibody. (E) Immunoblot analysis of the indicated cell extracts. (F) Immunoblot analysis of the indicated cell extracts following immunoprecipitation with IgG or anti-TNKS1 antibody. (G) Immunoblot analysis of transfected U2OS cells immunoprecipitated with anti-myc antibody. (H) Telomeric DNA ChIP analysis of HeLa cells transfected with vector, macroH2A1.1, or macroH2A1.2 using the indicated antibodies. (I) Quantification of the signal intensity of telomeric DNA immunoprecipitated by TNKS1 antibody. Average of two independent experiments ±SEM. (J) FISH analysis of vector, macroH2A1.1, or macroH2A1.2 transfected HeLa mitotic cells with a 16ptelo probe (green). DNA was stained with DAPI (blue). Scale bar, 5 μm. (K) Quantification of the frequency of mitotic cells with cohered telomeres. Average of two independent experiments, (n=41-53 cells each) ±SEM. (L) Immunoblot analysis of GM847 ALT cells following infection with GFP or macroH2A1 shRNA lentiviruses. (M) Quantification of the frequency of mitotic

cells with cohered telomeres from 16p FISH analysis of mitotic cells. Average of two independent experiments (n=50 cells each) ±SEM. *p≤0.05, **p≤0.01, students unpaired t-test. See also Figure S2.

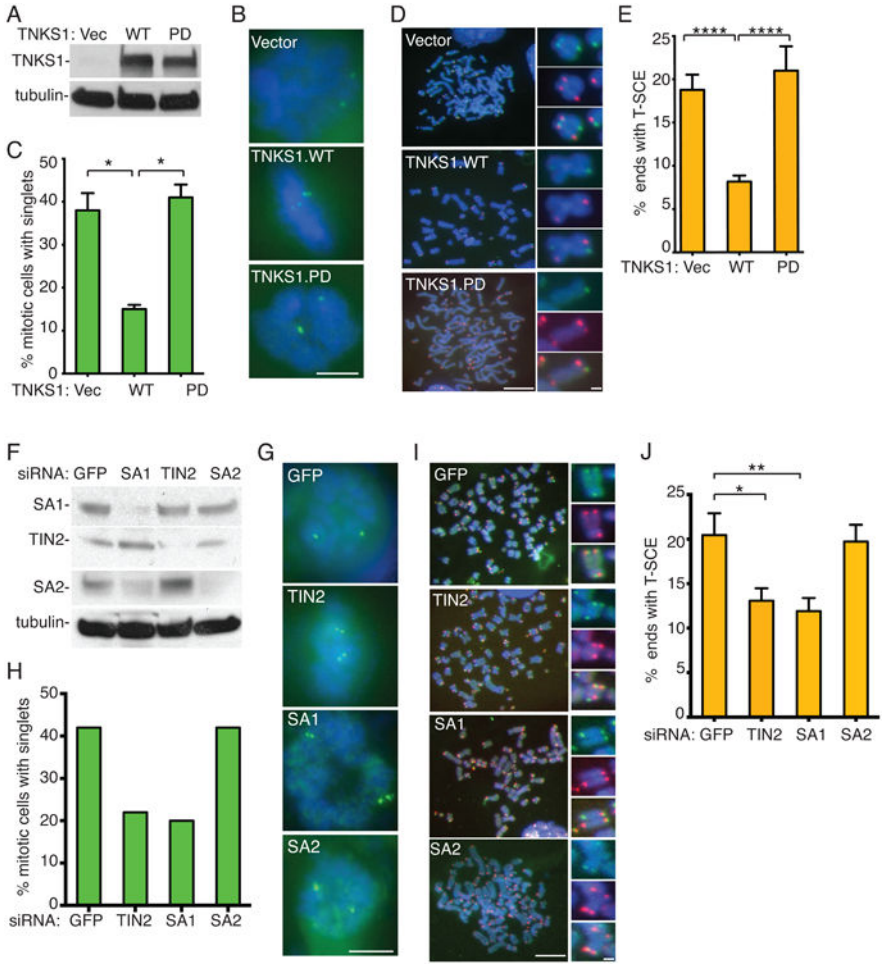

Figure 3.

Resolution of telomere cohesion represses sister telomere recombination in ALT cells. (A) Immunoblot analysis of U2OS cells stably expressing vector, TNKS1.WT or TNKS1.PD. (B, C) FISH analysis of mitotic cells with a 16ptelo probe (B, green) and quantification of the frequency of mitotic cells with cohered telomeres (C) of U2OS cells stably expressing vector, TNKS1.WT or TNKS1.PD. DNA was stained with DAPI (blue). Scale bar, 5 μm. Average of two independent experiments (n=49-51 cells each) ±SEM. (D, E) CO-FISH analysis of metaphase spreads probed with TTAGGG (red) and CCCTAA (green) (D) and quantification of the frequency of T-SCE (E) from vector, TNKS1.WT, or TNKS1.PD expressing U2OS cells. DNA was stained with DAPI (blue). Scale bar, 10 μm. Inset scale bar, 2 μm. Average of two independent experiments (n=684-1338 chromosomes each) ±SEM. (F) immunoblot analysis of U2OS cells transiently transfected with GFP, TIN2, SA1, or SA2 siRNA. (G, H) FISH analysis of mitotic cells with a 16ptelo probe (green) (G) and quantification of the frequency of mitotic cells with cohered telomeres (n=50 cells) (H) of U2OS cells transiently transfected with GFP, TIN2, SA1, or SA2 siRNA. DNA was stained with DAPI (blue). Scale bar, 5 μm. (I, J) CO-FISH analysis of metaphase spreads probed with TTAGGG (red) and CCCTAA (green) (I) and quantification of the frequency of T-SCE (J) of U2OS cells transiently transfected with GFP, TIN2, SA1, or SA2 siRNA. DNA was stained with DAPI (blue). Scale bar, 10 μm. Inset scale bar, 1 μm. Average of two

independent experiments (n=733-824 chromosomes each) ±SEM. *p≤0.05, **p≤0.01, ****p≤0.0001 students unpaired t-test.

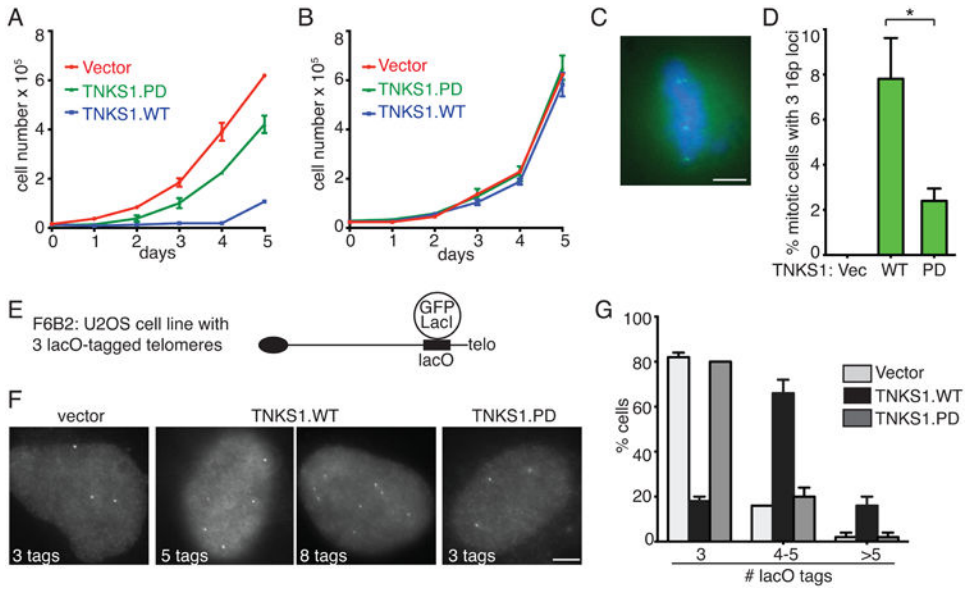

Figure 4.

Resolution of telomere cohesion impairs cell growth and induces inter-telomere recombination in ALT cells. (A, B) Growth curves of U2OS (A) and HeLa (B) cells infected with vector, TNKS1.WT, or TNKS1.PD lentivirus. Average of three technical replicates ±SD. (C) Example of a TNKS1.WT overexpressing U2OS cell with three 16p loci assayed by FISH with a 16ptelo probe (green). DNA was stained with DAPI (blue). Scale bar, 5 μm. (D) Quantification of the frequency of mitotic cells with three 16p telomeric loci. Average of two independent experiments (n=49-51 cells each) ±SEM. *p≤0.05 students unpaired t-test. (E) Schematic representation of the tagged U2OS cell line. (F) Detection of lacO tags by immunofluorescence with anti-GFP antibody of F6B2(U2OS-3lacO)/GFPLacI cells expressing vector, TNKS1.WT, or TNKS1.PD. Scale bar, 5 μm. (G) Quantification of the frequency of cells with the indicated number of tags. Average of two independent experiments (n=25 cells each) ±SEM. See also Figure S3.

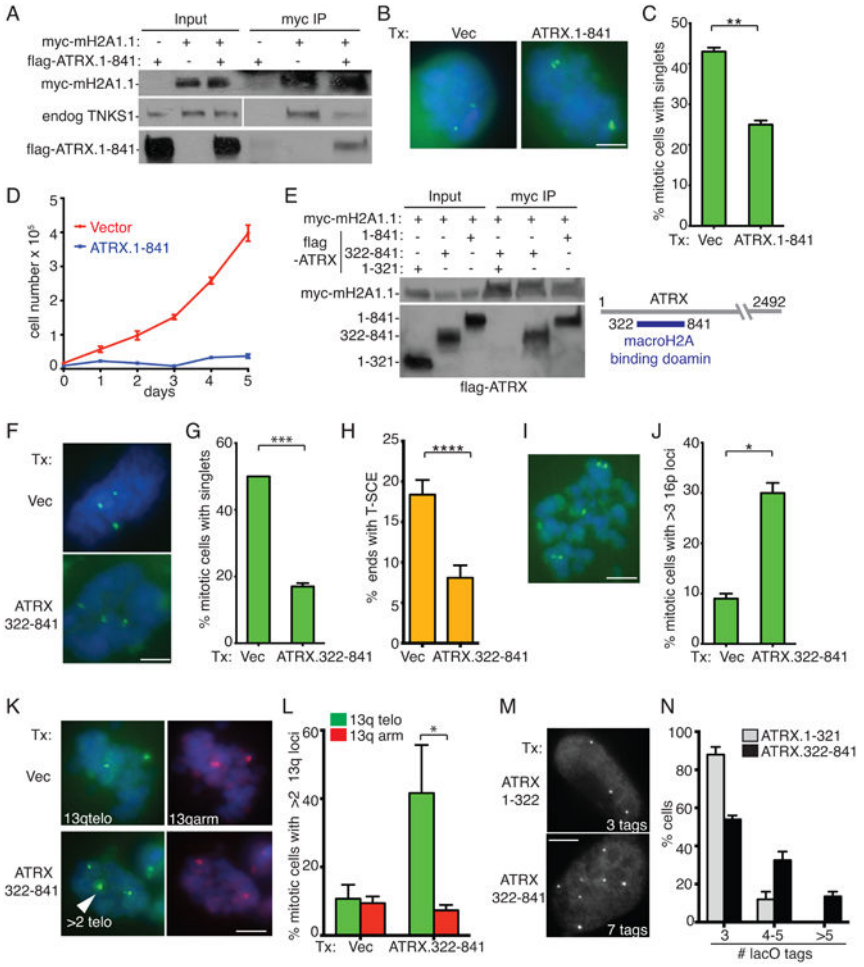

Figure 5.

The macroH2A-binding domain of ATRX induces resolution of telomere cohesion and inter-telomere recombination in ALT cells. (A) Immunoblot analysis of transfected U2OS cell extracts following immunoprecipitation with anti-myc antibody. (B) FISH analysis of mitotic U2OS cells transfected with vector or ATRX.1-841 using a 16ptelo probe (green). DNA was stained with DAPI (blue). Scale bar, 5 μm. (C) Quantification of the frequency of mitotic cells with cohered telomeres. Average of two independent experiments (n=25-50 cells each) ±SEM. (D) Growth curves of U2OS cells infected with vector or ATRX.1-841 lentivirus. Average of three technical replicates ±SD. (E) Immunoblot analysis of transfected GM847 cell extracts following immunoprecipitation with anti-myc antibody. (F) FISH analysis of mitotic GM847 cells transfected with vector or ATRX.322-841 with a 16ptelo probe (green). DNA was stained with DAPI (blue). Scale bar, 5 μm. (G) Quantification of the frequency of mitotic cells with cohered telomeres. Average of two independent experiments (n=50 cells each) ±SEM. (H) Quantification of the frequency of T-SCE from CO-FISH analysis of metaphase spreads from U2OS cells stably expressing vector and ATRX.322-841. Average of two independent experiments (n=124-638 chromosomes each) ±SEM. (I) Example of an ATRX.322-841 overexpressing GM847 cell with four 16p loci assayed by FISH with a 16ptelo probe (green). DNA was stained with DAPI (blue). Scale bar, 5 μm. (J) Quantification of the frequency of mitotic cells with more than three 16p

telomeric loci. Average of two independent experiments (n=50 cells each) ±SEM. (K) Dual FISH analysis of mitotic GM847 cells transfected with vector or ATRX.322-841 with a 13qtelo (green) and arm (red) probe. DNA was stained with DAPI (blue). Scale bar, 5 μm. (L) Quantification of the frequency of mitotic cells with more than two 13q telo and arm loci. Average of 3 independent experiments (n=11-26 cells each) ±SD. (M) Immunofluorescence analysis of analysis of lacO tags in F6B2(U2OS-3lacO) cells transfected with GFPLacI and ATRX.1-321 or ATRX.322-841. Scale bar, 5 μm. (N) Quantification of the frequency of cells with the indicated number of tags. Average of two independent experiments (n=25 cells each) ±SEM. *p≤0.05, **p≤0.01, ***p≤0.0001, ****p≤0.0001, students unpaired t-test. See also Figure S4.

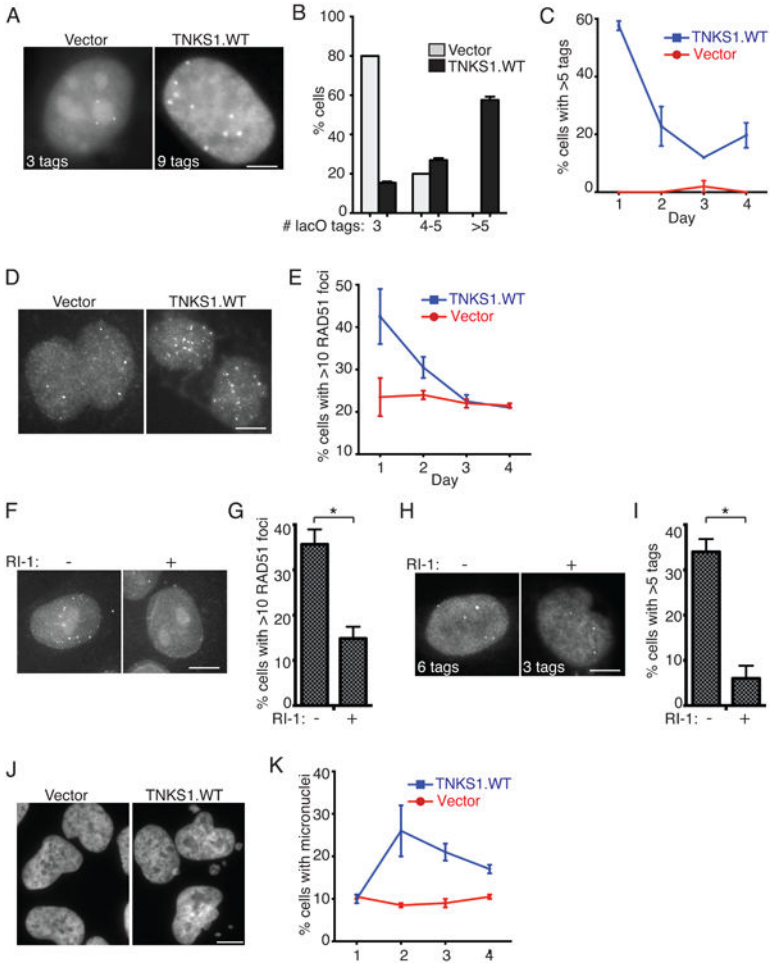

Figure 6.

Resolution of telomere cohesion leads to immediate, rampant recombination and genomic instability. (A, B) Detection of lacO tags by immunofluorescence with anti-GFP antibody (A) and quantification of the frequency of cells with the indicated number of tags (B) in F6B2(U2OS-3lacO)/GFPLacI cells following infection with vector or TNKS1.WT lentivirus on Day 1. Scale bar, 5 μm. Average of two independent experiments (n=25 cells each) ±SEM. (C) Quantification of the frequency of F6B2(U2OS-3lacO)/GFPLacI cells following infection with vector or TNKS1.WT lentivirus displaying more than 5 tags on days 1-4. Average of two independent experiments (n=25 cells each) ±SEM. (D, E) Detection of RAD51 foci by immunofluorescence analysis on Day 1 (D) and quantification of the frequency of cells displaying more than 10 RAD51 foci on days 1-4 (E) in U2OS cells following infection with vector or TNKS1.WT lentivirus. Scale bar, 10 μm. Average of two independent experiments (n=100 cells each) ±SEM. (F, G) Detection of RAD51 foci by immunofluorescence analysis (F) and quantification of the frequency of cells displaying more than 10 RAD51 foci (G) in U2OS cells on Day 1 following infection with TNKS1.WT lentivirus. Cells were treated with RAD51 inhibitor RI-1 for 8 hr prior to harvest. Scale bar, 10 μm. Average of two independent experiments (n=100 cells each) ±SEM. (H, I) Detection of lacO tags by immunofluorescence with anti-GFP antibody (H) and quantification of the frequency of cells with the indicated number of tags (I) in F6B2(U2OS-3lacO)/GFPLacI

cells on Day 1 following infection with TNKS1.WT lentivirus. Cells were treated with RAD51 inhibitor RI-1 for 8 hr prior to harvest. Scale bar, 10 μm. Average of two independent experiments (n=25 cells each) ±SEM. *p≤0.05 students unpaired t-test. (J, K) Detection of micronuclei by immunofluorescence staining with DAPI on Day 2 (J) and quantification of the frequency of micronucleation events on days 1-4 (K) in U2OS cells following infection with vector or TNKS1.WT lentivirus. Scale bar, 10 μm. Average of two independent experiments (n=100 cells each) ±SEM. See also Figure S5.

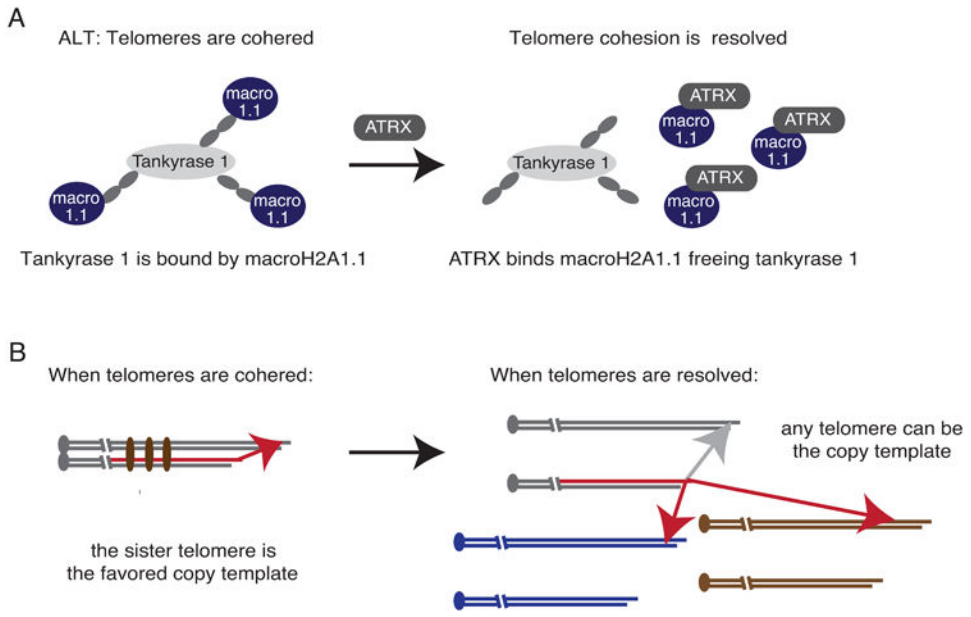

Figure 7.

Model for the role of persistent telomere cohesion in ALT. (A) Loss of ATRX in ALT frees macroH2A1.1 to bind and sequester tankyrase 1 thereby preventing resolution of sister telomere cohesion. When ATRX is reintroduced into ALT cells it binds macroH2A1.1, freeing tankyrase 1 to resolve telomere cohesion. (B) When telomeres are cohered the sister telomere is the favored copy template. Upon forced resolution of telomere cohesion in ALT cells (by introduction of ATRX, overexpression of tankyrase 1, or depletion of macroH2A1.1) any telomere can be the copy template.